QUARTERLY OF APPLIED MATHEMATICS
OCTOBER 1979

# GLOBAL ANALYSIS OF MAGNETIC DOMAINS*

BY

W. L. MIRANKER AND B. E. WILLNER

*IBM Thomas J. Watson Research Center, Yorktown Heights*

**Abstract.** We study the phase transition problem for ferromagnetic materials. By means of examples we show that a mathematical bifurcation process may be used to describe the evolution of one configuration of magnetic domains into another.

**1. Introduction.** The study of the magnetization of anisotropic ferromagnetic materials (cf. [1, 5]) has acquired increased interest because of the invention of magnetic bubble devices (cf. [2, 3, 6]). Such materials are typically composed of regions in which the magnetization is approximately uniform. These regions of near-uniformity are called magnetic domains. Between domains there are transition layers in which the magnetization changes abruptly. These transition layers are called domain walls. (For example, a magnetic bubble is a cylindrical domain in a thin film of magnetic material.)

We will use the term specimen to denote the sample of magnetic material in question as well as the region of space which the sample occupies. The latter will also be denoted by the symbol $\Omega$. Let $\mathbf{M}$ be the magnetization as a function of position in the specimen. The specimen is taken as magnetically saturated so that

$$\mathbf{M} = M_s \boldsymbol{\nu},$$

where $M_s$ is a constant and $\boldsymbol{\nu}$ is a unit vector.

The microscopic theory of magnetization in these materials begins with a description of the energy density. The latter is composed of four terms, each of which is a function of the magnetization. The four energy densities are

i) anisotropy energy density
ii) applied field energy density
iii) exchange energy density
iv) self field energy density.

The total energy consists of the integral over the specimen, $\Omega$, of the sum of these four densities. Functions $\mathbf{M}$ for which the total energy has a relative minimum are taken as the physically realizable states of magnetization. Thus, the determination of the magnetization corresponds to solving a variational problem for $\mathbf{M}$; namely, the minimization of the total energy.

A specimen may exist in many different configurations of magnetic domains. Correspondingly, we may expect that the variational problem has many solutions. The object of

* Received September 7, 1978. The authors are grateful to M. Freiser, Y. Lin, C. C. Shir and J. Slonczewski for helpful discussions.

this paper is to show how some of these different configurations arise, including as well a mathematical mechanism describing the evolution of one configuration into another. We do this by means of a bifurcation process and, in particular, by solving two examples. A limitation of our results is that some of the solutions which we produce, while describing domain configurations, domain walls, etc., are in fact unstable. That is, the solutions of the variational problem which they represent are saddle points rather than relative minima. This limitation is probably due to the univariate character of our examples (a feature which we have adopted in order to achieve complete solvability). We hope to deal with more involved examples in forthcoming work.

In Sec. 2 we derive the mathematical model as the Euler equations of the variational problem for **M**. In Sec. 3 we nondimensionalize the problem and characterize it in terms of two nondimensional material parameters. In Sec. 4 we study two examples of magnetic films. Utilizing the form of the model derived in Sec. 3, we give a global analysis of the problem showing how the various solutions appear and disappear as parameters change. This bifurcation process shows that these solutions have the character of magnetic domains separated by domain walls.

**2. The mathematical model.** In this section we will introduce the energy as the integral over the specimen of the sum of the four energy densities. Then we will perform a variation to obtain the equations governing the magnetization **M**.

*Coordinates for* $\boldsymbol{\nu}$. Since the specimen is assumed magnetically saturated, the magnetization can be written as

$$\mathbf{M} = M_s \boldsymbol{\nu}, \tag{2.1}$$

where $M_s$ is a material parameter and $\boldsymbol{\nu}$ is a unit vector. Our specimens will be homogeneous so that $M_s$ is a constant. We represent the unit vector $\boldsymbol{\nu} = (\nu_x, \nu_y, \nu_z)$ in standard spherical coordinates, viz.

$$\nu_x = \cos\theta \sin\phi, \quad \nu_y = \sin\theta \sin\phi, \quad \nu_z = \cos\phi. \tag{2.2}$$

*Energy densities.* We will now define the four energy densities.

(i) *Anisotropy energy.* One component of the internal energy density is due to the anisotropic nature of the material and is a function of the local orientation of the magnetization. This component which is called the anisotropy energy density is given by

$$\rho_{anisotropy} = kf(\theta,\phi), \tag{2.3}$$

where $k$ is a measure of the strength of the anisotropy and $f(\theta, \phi)$ describes how this energy depends on the orientation of **M** relative to a coordinate system fixed in the material. Both $k$ and $f(\theta,\phi)$ are material-dependent. (Examples of the function $f(\theta, \phi)$ will be given in Sec. 4.)

(ii) *Applied field energy.* If the specimen is in the presence of an applied field $\mathbf{H}_a$, it has a potential energy density due to this field given by

$$\rho_{applied} = -\mathbf{M} \cdot \mathbf{H}_a . \tag{2.4}$$

(iii) *Exchange energy.* Another material property is the existence of a force which acts to align the magnetization on a molecular level. This force depends on the rate of spatial variation of **M** but not on its orientation. The corresponding energy density is called the

exchange energy density and is given by

$$\rho_{exchange} = \frac{1}{2}c(|\nabla v_x|^2 + |\nabla v_y|^2 + |\nabla v_z|^2), \tag{2.5}$$

where $c$ is a material parameter measuring the magnitude of these exchange forces. Using (2.2) this may be written as

$$\rho_{exchange} = \frac{1}{2}c(|\nabla\phi|^2 + \sin^2\phi|\nabla\theta|^2). \tag{2.6}$$

(iv) *Self-field energy.* The magnetization M itself generates a field called the self-field, $\mathbf{H}_s$. The potential energy due to $\mathbf{H}_s$ is called the self-field energy and its density is given by

$$\rho_{self} = -\frac{1}{2}\mathbf{M}\cdot\mathbf{H}_s. \tag{2.7}$$

*The total energy and its variation.* The total energy $E_{Tot}$ is obtained by adding the four energy densities just introduced and integrating the sum over the specimen, $\Omega$:

$$E_{Tot} = \int_\Omega \left[kf(\theta,\phi) - \mathbf{M}\cdot\mathbf{H}_a + \frac{1}{2}c(|\nabla\phi|^2 + \sin^2\phi|\nabla\theta|^2) - \frac{1}{2}\mathbf{M}\cdot\mathbf{H}_s\right] d\Omega, \tag{2.8}$$

where $d\Omega$ denotes the volume element.

We will show that the variation $\delta E_{Tot}$ with respect to variations $\delta\theta$ and $\delta\phi$ of $\theta$ and $\phi$ respectively is

$$\begin{aligned}\delta E_{Tot} = &\int_\Omega \delta\phi\left[k\frac{\partial f}{\partial\phi} - M_s\frac{\partial \boldsymbol{\nu}}{\partial\phi}\cdot(\mathbf{H}_a + \mathbf{H}_s) + c\sin\phi\cos\phi|\nabla\theta|^2 - c\nabla^2\phi\right] d\Omega\\ &+ \int_\Omega \delta\theta\left[k\frac{\partial f}{\partial\theta} - M_s\frac{\partial \boldsymbol{\nu}}{\partial\theta}\cdot(\mathbf{H}_a + \mathbf{H}_s) - 2c\sin\phi\cos\phi\nabla\phi\cdot\nabla\theta - c\sin^2\phi\nabla^2\theta\right] d\Omega\\ &- c\int_{2\Omega}\delta\phi\nabla\phi\cdot\mathbf{n}dA + c\int_{2\Omega}\delta\theta\sin^2\phi\nabla\theta\cdot\mathbf{n}dA.\end{aligned} \tag{2.9}$$

$dA$ denotes the surface element on the boundary, $\partial\Omega$, of $\Omega$, and $\mathbf{n}$ denotes the outwardly-directed unit normal vector to $\Omega$.

To show (2.9) we treat the four contributions to the energy in turn. Thus

$$E_{anisotropy} = \int_\Omega \rho_{anisotropy}\, d\Omega = \int_\Omega kf(\theta,\phi)d\Omega, \tag{2.10}$$

and

$$\delta E_{anisotropy} = \int_\Omega k\left(\delta\theta\frac{\partial f}{\partial\theta} + \delta\phi\frac{\partial f}{\partial\theta}\right)d\Omega. \tag{2.11}$$

Similarly,

$$E_{applied} = \int_{\Omega} \rho_{applied}\, d\Omega = -\int_{\Omega} M_s \boldsymbol{\nu} \cdot \mathbf{H}_a d\Omega. \tag{2.12}$$

Thus

$$\delta E_{applied} = -\int_{\Omega} M_s \left( \delta\theta \frac{\partial \boldsymbol{\nu}}{\partial \theta} \cdot \mathbf{H}_a + \delta\phi \frac{\partial \boldsymbol{\nu}}{\partial \phi} \cdot \mathbf{H}_a \right) d\Omega. \tag{2.13}$$

To continue we note that to the variations $\delta\theta$ and $\delta\phi$ there correspond variations $\delta\mathbf{M}$ and $\delta\mathbf{H}_s$ in $\mathbf{M}$ and $\mathbf{H}_s$ respectively. Then

$$E_{self} = \int_{\Omega} \rho_{self}\, d\Omega = -\frac{1}{2} \int_{\Omega} \mathbf{M} \cdot \mathbf{H}_s d\Omega. \tag{2.14}$$

Then

$$\delta E_{self} = -\frac{1}{2} \int_{\Omega} \delta\mathbf{M} \cdot \mathbf{H}_s d\Omega - \frac{1}{2} \int_{\Omega} \mathbf{M} \cdot \delta\mathbf{H}_s d\Omega = -\int_{\Omega} \delta\mathbf{M} \cdot \mathbf{H}_s d\Omega, \tag{2.15}$$

the latter following from Green's reciprocity formula (cf. [4, p. 51]).

Then

$$\delta E_{self} = -\int_{\Omega} M_s \left( \delta\theta \frac{\partial \boldsymbol{\nu}}{\partial \theta} \cdot \mathbf{H}_s + \delta\phi \frac{\partial \boldsymbol{\nu}}{\partial \phi} \cdot \mathbf{H}_s \right) d\Omega. \tag{2.16}$$

Lastly we have

$$E_{exchange} = \int_{\Omega} \rho_{exchange} d\Omega = \frac{1}{2} \int_{\Omega} c(|\nabla\phi|^2 + \sin^2\phi |\nabla\theta|^2) d\Omega. \tag{2.17}$$

Then

$$\delta E_{exchange} = c \int_{\Omega} [\nabla\phi \cdot \nabla\delta\phi + \sin\phi \cos\phi |\nabla\theta|^2 \delta\phi + \sin^2\phi (\nabla\theta \cdot \nabla\delta\theta)] d\Omega. \tag{2.18}$$

Eq. (2.18) may be written more conveniently as

$$\begin{aligned} \delta E_{exchange} = {} & c \int_{\Omega} \sin\phi \cos\phi |\nabla\theta|^2 \delta\phi d\Omega + c \int_{\Omega} \nabla \cdot (\delta\phi \nabla\phi) d\Omega \\ & - c \int_{\Omega} \delta\phi \nabla^2\phi d\Omega + c \int_{\Omega} \nabla \cdot (\delta\theta \sin^2\phi \nabla\theta) d\Omega - c \int_{\Omega} \delta\theta (\nabla \cdot \sin^2\phi \nabla\theta) d\Omega. \end{aligned} \tag{2.19}$$

In this form we may apply the divergence theorem to obtain finally

$$\delta E_{exchange} = c\int_{\Omega}\delta\phi(\sin\phi\cos\phi|\nabla\theta|^2-\nabla^2\phi)d\Omega$$
$$+ c\int_{\Omega}\delta\theta(-2\sin\phi\cos\phi\nabla\phi\cdot\nabla\theta-\sin^2\phi\nabla^2\theta)d\Omega$$
$$+ c\int_{\Omega}\delta\phi(\nabla\phi\cdot\mathbf{n})dA + c\int_{\Omega}\delta\theta(\sin^2\phi\nabla\theta\cdot\mathbf{n})dA. \tag{2.20}$$

Here $\mathbf{n}$ is the outwardly-directed unit normal vector to $\Omega$.

Eqs. (2.11), (2.13), (2.16) and (2.20) taken together demonstrate the claimed form (2.9) for $\delta E_{Tot}$.

*Equations of equilibrium.* Setting the first variation of $E_{Tot}$ to zero, we produce the following necessary conditions for static equilibrium:

$$\nabla^2\phi - c\sin\phi\cos\phi\,|\nabla\theta|^2 + M_s(\mathbf{H}_a + \mathbf{H}_s)\cdot\frac{\partial\boldsymbol{\nu}}{\partial\phi} - k\frac{\partial f}{\partial\phi} = 0, \tag{2.21}$$

$$c\sin^2\phi\nabla^2\theta + 2c\sin\phi\cos\phi\nabla\phi\cdot\nabla\theta + M_s(\mathbf{H}_a+\mathbf{H}_s)\cdot\frac{\partial\boldsymbol{\nu}}{\partial\theta} - k\frac{\partial f}{\partial\theta} = 0 \tag{2.22}$$

and

$$c\nabla\phi\cdot\mathbf{n} = 0, \qquad c\sin^2\theta\nabla\theta\cdot\mathbf{n} = 0. \tag{2.23}$$

The differential equations (2.21) and (2.22) are valid in the specimen, $\Omega$, while the boundary conditions (2.23) apply on $\partial\Omega$.

*The self field.* The self field $\mathbf{H}_s$ occurring in the equations of equilibrium (2.21) and (2.22) is itself a function of the orientation of the magnetization $\boldsymbol{\nu}$ (i.e. of $\theta$ and $\phi$). We now derive conditions for determining $\mathbf{H}_s = \mathbf{H}_s(\boldsymbol{\nu})$.

Let $\mathbf{B}_s$ be the magnetic induction corresponding to the magnetic field $\mathbf{H}_s$ and magnetization $\mathbf{M}$. Maxwell's equations are

$$\nabla\cdot\mathbf{B}_s = 0, \qquad \nabla\times\mathbf{H}_s = 0, \tag{2.24, 2.25}$$

where

$$\mathbf{B}_s = \mathbf{H}_s + 4\pi\mathbf{M}. \tag{2.26}$$

Defining $\mathbf{M}$ to be identically zero outside of $\Omega$, these equations are valid everywhere.

It follows from (2.24) and (2.26) that

$$\nabla\cdot\mathbf{H}_s = -4\pi\nabla\cdot\mathbf{M}, \tag{2.27}$$

everywhere, except possibly on $\partial\Omega$ where $\mathbf{M}$ and $\mathbf{H}_s$ may be discontinuous. On the boundary, $\partial\Omega$, (2.24) shows that the normal component of $\mathbf{B}_s$ (i.e. $\mathbf{B}_s\cdot\mathbf{n}$) is continuous. Thus from (2.26) we have

$$(\mathbf{H}_s + 4\pi\mathbf{M})\cdot\mathbf{n}|_{\partial\Omega^-} = \mathbf{H}_s\cdot\mathbf{n}|_{\partial\Omega^+}. \tag{2.28}$$

Here $\partial\Omega^{\pm}$ denotes a point on $\partial\Omega$ approached from outside respectively inside of $\Omega$.

Eq. (2.25) allows us to express $\mathbf{H}_s$ as the gradient of a scalar potential $u$, i.e.

$$\mathbf{H}_s = -\nabla u. \tag{2.29}$$

Combining (2.27), (2.28) and (2.29), we obtain the following boundary value problem for $u$ (i.e. for the specification $H_s$):

$$\nabla^2 u = 4\pi \nabla \cdot \mathbf{M}, \tag{2.30}$$

$$\left(-\frac{\partial u}{\partial \mathbf{n}} + 4\pi \mathbf{M} \cdot \mathbf{n}\right)\Big|_{\partial\Omega^-} = -\frac{\partial u}{\partial \mathbf{n}}\Big|_{\partial\Omega^+}. \tag{2.31}$$

Recall $\mathbf{M}$ is taken to be zero outside of $\Omega$ so that (2.30) is valid everywhere, except on $\partial\Omega$ where (2.31) holds. This boundary value problem is augmented by the condition at infinity that $u$ behaves like the fundamental solution for the Laplace operator, i.e.

$$u = O(r^{-1}). \tag{2.32}$$

Here $r$ is distance measured from some fixed point.

The solution of the boundary value problem (2.29)–(2.31) may be written as follows:

$$u(r) = \int_\Omega \frac{-\nabla \cdot \mathbf{M}}{|\mathbf{r} - \mathbf{r}'|}\, d\Omega + \int_\Omega \frac{\mathbf{M} \cdot n}{|\mathbf{r} - \mathbf{r}'|}\, dA. \tag{2.33}$$

Introducing the linear operator $\mathscr{K}(\mathbf{M})$ by

$$\mathscr{K}(\mathbf{M}) = -\int_\Omega (\nabla \cdot \mathbf{M})\left(\nabla \frac{1}{|\mathbf{r} - \mathbf{r}'|}\right) d\Omega + \int_\Omega (\mathbf{M} \cdot \mathbf{n})\left(\nabla \frac{1}{|\mathbf{r} - \mathbf{r}'|}\right) dA, \tag{2.34}$$

we may write $\mathbf{H}_s(\mathbf{r})$ as

$$\mathbf{H}_s(\mathbf{r}) = \mathscr{K}(\mathbf{M}). \tag{2.35}$$

The mathematical model for $\mathbf{M}$ is now derived. It consists of the boundary value problem (2.21)–(2.23) for $\nu$ coupled with the expression (2.35) for the self field $\mathbf{H}_s$ in terms of $\mathbf{M}$.

*Second variation.* A sufficient condition for a solution $(\theta, \phi)$ of the model to be a local minimum of $E_{Tot}$ is that the second variation $\delta^2 E_{Tot}$ be positive for all nonzero variation $(\delta\theta, \delta\phi)$.

We find that

$$\begin{aligned}
\delta^2 E_{Tot} = \int_\Omega \Big\{ & k\left[\frac{1}{2} f_{\theta\theta}(\delta\theta)^2 + f_{\theta\phi}\delta\theta\delta\phi + \frac{1}{2} f_{\phi\phi}(\delta\phi)^2\right] \\
& - M_s\Big[\mathbf{H}_a \cdot \left(\frac{1}{2}\nu_{\theta\theta}(\delta\theta)^2 + \nu_{\theta\phi}\delta\theta\delta\phi + \frac{1}{2}\nu_{\phi\phi}(\delta\phi)^2\right) \\
& + \frac{1}{2}\mathscr{K}(\nu_\theta\delta\theta + \nu_\phi\delta\phi) \cdot (\nu_\theta\delta\theta + \nu_\phi\delta\phi) \\
& + \left(\frac{1}{2}\nu_{\theta\theta}(\delta\theta)^2 + \nu_{\theta\phi}\delta\theta\delta\phi + \frac{1}{2}\nu_{\phi\phi}(\delta\phi)^2\right) \cdot \mathscr{K}(\nu)\Big]
\end{aligned}$$

$$+ \frac{1}{2} c[(\nabla\delta\phi)^2 + |\nabla\theta|^2((\delta\phi)^2 \cos 2\phi)$$

$$+ 2(\nabla\theta \cdot \nabla\delta\theta)(\delta\phi \sin 2\phi) + \sin^2\phi|\nabla\delta\theta|^2]\Big\} d\Omega. \tag{2.36}$$

Here all function arguments are $(\theta, \phi)$.

**3. Nondimensionalization.** In a specimen occupying a fixed domain $\Omega$, having a prescribed anisotropy $f(\theta, \phi)$ and subjected to a specified magnetic field $\mathbf{H}_a$, the magnetization $\mathbf{M}$ is a function of the position vector $\mathbf{r}$ and the material parameters $M_s$, $k$ and $c$. In this section we will cast the problem in a nondimensional form. In this form the nondimensional magnetization $\boldsymbol{\nu}$ is a function of a nondimensional position vector $\sigma$ and the two dimensionless material parameters $\lambda$ and $\mu$.

We introduce the following nondimensional variables: magnetic field $\mathbf{h}_a$ and $\mathbf{h}_s$; potential $w$; position vector $\sigma$; parameters $\lambda$, $\mu$ by means of the following relations:

$$\mathbf{H}_a = M_s\mathbf{h}_a, \qquad \mathbf{H}_s = M_s\mathbf{h}_s, \tag{3.1, 3.2}$$

$$u = lM_s w, \qquad \mathbf{r} = l\sigma, \tag{3.3, 3.4}$$

$$\lambda = l^2k/c, \qquad \mu = l^2M_s^2/c. \tag{3.5, 3.6}$$

Here $l$ is a characteristic specimen length in physical units and, although the specimen is now in $\sigma$-coordinates, we still use $\Omega$ and $\partial\Omega$ to denote it and its boundary.

The boundary value problem (2.21)–(2.23) takes on the following nondimensional form:

$$\nabla^2\phi - \sin\phi\cos\phi|\nabla\theta|^2 + \mu(\boldsymbol{h}_a + \boldsymbol{h}_s) \cdot \frac{\partial \boldsymbol{\nu}}{\partial\phi} - \lambda\frac{\partial f}{\partial\phi} = 0, \tag{3.7}$$

$$\sin^2\phi\nabla^2\theta + 2\sin\phi\cos\phi\nabla\phi \cdot \nabla\theta + \mu(\mathbf{h}_a + \mathbf{h}_s) \cdot \frac{\partial \boldsymbol{\nu}}{\partial\theta} - \lambda\frac{\partial f}{\partial\theta} = 0 \tag{3.8}$$

for $\sigma \in \Omega$, and

$$\nabla\phi \cdot \mathbf{n} = 0, \qquad \sin^2\phi\nabla\theta \cdot \mathbf{n} = 0 \tag{3.9}$$

for $\sigma \in \partial\Omega$.

The potential problem (2.29)–(2.32) becomes

$$\mathbf{h}_s = -\nabla w, \tag{3.10}$$

$$\nabla^2 w = 4\pi\nabla \cdot \boldsymbol{\nu}, \tag{3.11}$$

$$\left(-\frac{\partial w}{\partial \mathbf{n}} + 4\pi\boldsymbol{\nu} \cdot \mathbf{n}\right)\Big|_{\partial\Omega^-} = -\frac{\partial w}{\partial \mathbf{n}}\Big|_{\partial\Omega^+}. \tag{3.12}$$

Here and hereafter the operators $\nabla$ and $\partial/\partial\mathbf{n}$ and the vector $\mathbf{n}$ are in terms of the dimensionless position variable $\sigma$. Referring to (2.35), the solution of this potential problem may be written as

$$\mathbf{h}_s(\sigma) = \mathscr{H}(\boldsymbol{\nu}). \tag{3.13}$$

*Second variation.* In terms of the non-dimensional variables introduced here the condition for the positivity of $\delta^2 E_{Tot}$ becomes (cf. (2.36)):

$$
\begin{aligned}
0 < \int_\Omega \lambda \Big[ & \frac{1}{2} f_{\theta\theta}(\delta\theta)^2 + \delta_{\theta\phi}\delta\theta\delta\phi + \frac{1}{2} f_{\phi\phi}(\delta\phi)^2 \Big] \\
& - \mu \Big[ \mathbf{h}_a \cdot \Big( \frac{1}{2} \boldsymbol{\nu}_{\theta\theta}(\delta\theta)^2 + \boldsymbol{\nu}_{\theta\phi}\delta\theta\delta\phi + \frac{1}{2} \boldsymbol{\nu}_{\phi\phi}(\delta\phi)^2 \Big) \\
& + \frac{1}{2} \mathscr{H}(\boldsymbol{\nu}_\theta \delta\theta + \boldsymbol{\nu}_\phi \delta\phi) \cdot (\boldsymbol{\nu}_a \delta\theta + \boldsymbol{\nu}_\phi \delta\phi) \\
& + \Big( \frac{1}{2} \boldsymbol{\nu}_{\theta\theta}(\delta\theta)^2 + \boldsymbol{\nu}_{\theta\phi}\delta\theta\delta\phi + \frac{1}{2} \boldsymbol{\nu}_{\phi\phi}(\delta\phi)^2 \Big) \cdot \mathscr{H}(\boldsymbol{\nu}) \Big] \\
& + \frac{1}{2} \Big[ (\nabla\delta\phi)^2 + |\nabla\theta|^2((\delta\phi)^2 \cos 2\phi) \\
& + 2(\nabla\theta \cdot \nabla\delta\theta)(\delta\phi \sin 2\phi) + \sin^2\phi |\nabla\delta\phi|^2 \Big] \Big) \, d\Omega. \qquad (3.14)
\end{aligned}
$$

We will abbreviate this condition by calling the right member $\delta^2 \bar{E}_{Tot}$.

**4. Univariate examples.** We treat two examples in which the boundary value problem may be analyzed completely.

Example 1: we choose $f = \nu_z^2 + \gamma \nu_y^2$. This is a case in which the $y$ and $z$ directions are hard axes of magnetization with $\gamma$ measuring a bias with respect to this property.

Examples 2: we consider a uniaxial anisotropy modeling a film of magnetic material which has been doped by ionic bombardment. The anisotropy which varies across the film is modeled by a lamination of two uniform films.

*Specimen description.* Setting $\sigma = (x, y, z)$, the specimen occupies the region of space

$$\Omega = \{(x, y, z) | x \in [-1, 1], y \in (-\infty, \infty), z \in (-\infty, \infty)\}. \qquad (4.1)$$

This leads us to seek solutions which depend only on $x$, viz:

$$\boldsymbol{\nu} = \boldsymbol{\nu}(x) \qquad (4.2)$$

For this $\Omega$ and these solutions, the self field $\mathbf{h}_s$ is calculable in closed form.

*Self field.* Consider the specimen to be composed of planes orthogonal to the $x$-axis. To the surface planes $x = \pm 1$ we associate the uniform charge density $\pm \nu_x(\pm 1)$ respectively. To an interior plane we associate a volume charge density $-\nabla \cdot \boldsymbol{\nu} = -(\partial/\partial x)\nu_x$. Then the self field is seen to be

$$\mathbf{h}_s = 2\pi \Big[ -\nu_x(-1) - \int_{-1}^{x} \frac{\partial \nu_x}{\partial x} \, dx - \Big( \nu_x(1) - \int_x^1 \frac{\partial \nu_x}{\partial x} \, dx \Big) \Big] = -2\pi \nu_x. \qquad (4.3)$$

*Example* 1. In this example we take

$$f(\theta, \phi) = \cos^2\phi + \gamma \sin^2\theta \sin^2\phi, \qquad (4.4)$$

where $\gamma$ is a material parameter. Using (4.1)–(4.3), the boundary value problem (3.7)–

(3.9) becomes

$$\frac{d^2\phi}{dx^2} - \frac{1}{2}\sin 2\phi\left(\frac{d\theta}{dx}\right)^2 - \pi\mu\cos^2\theta\sin 2\phi - \lambda(\gamma\sin^2\theta - 1)\sin 2\phi = 0, \tag{4.5}$$

$$\sin^2\phi\frac{d^2\theta}{dx^2} + \sin 2\phi\theta_x\phi_x + \pi\mu\sin 2\theta\sin^2\phi - \lambda\gamma\sin 2\theta\sin^2\phi = 0, \tag{4.6}$$

with

$$d\phi/dx = 0 \quad \text{and} \quad \sin^2\phi(d\theta/dx) = 0, \quad x = \pm 1. \tag{4.7}$$

This boundary value problem has solutions of the form

$$\text{i) } \theta = 0, \qquad \text{ii) } \theta = \frac{\pi}{2}, \qquad \text{iii) } \theta = \pi, \tag{4.8}$$

with corresponding functions $\phi_i(x)$, $i = 1, 2, 3$. The $\phi_i$ are solutions of the following boundary value problem, respectively:

$$\frac{d\phi_i}{dx^2} - b_i\sin 2\phi_i = 0, \qquad \frac{d\phi_i(\pm 1)}{dx} = 0, \qquad i = 1, 2, 3. \tag{4.9}$$

Here

$$b_1 = b_3 = \pi\mu - \lambda, \qquad b_2 = \lambda(\gamma - 1). \tag{4.10}$$

We may drop the subscript $i$ in (4.9) and consider the case $b > 0$. For the case $b < 0$, we simply replace $\phi$ by $\phi + (\pi/2)$, while the case $b = 0$ corresponds to the solution $\phi =$ constant. In the problem for the case $b > 0$ we make the change of variables

$$\xi = b^{1/2}x. \tag{4.11}$$

The resulting boundary value problem is

$$\frac{d^2\phi}{d\xi^2} - \sin 2\phi = 0, \qquad \frac{d\phi(\pm b^{1/2})}{d\xi} = 0. \tag{4.12}$$

Let

$$L_b = 2b^{1/2}. \tag{4.13}$$

$L_b$ is the length of the interval on which the boundary value problem (4.12) is defined.

We begin our study of this boundary value problem by displaying a portion of the $(\phi, \phi_\xi)$-phase plane for the differential equation in (4.12) (see Fig. 4.1). The trajectory $T_1$ from $A$ to $B$ is a solution of the boundary value problem (4.12) when

$$L_b = \oint_{T_1} d\xi = \int_A^{\pi - A} \frac{d\phi}{(\cos 2\phi - \cos 2A)^{1/2}} \tag{4.14}$$

Indeed, every trajectory of the type $T_1$, that is, those which emanate from the interval $[0, \pi/2]$ on the $\phi$ axis in Fig. 4.1, is a corresponding such solution. The separatrix $S_1$ which emanates from $\phi = 0$ corresponds to $L_b = \infty$. The limiting value of $L_b$ to which these tra-

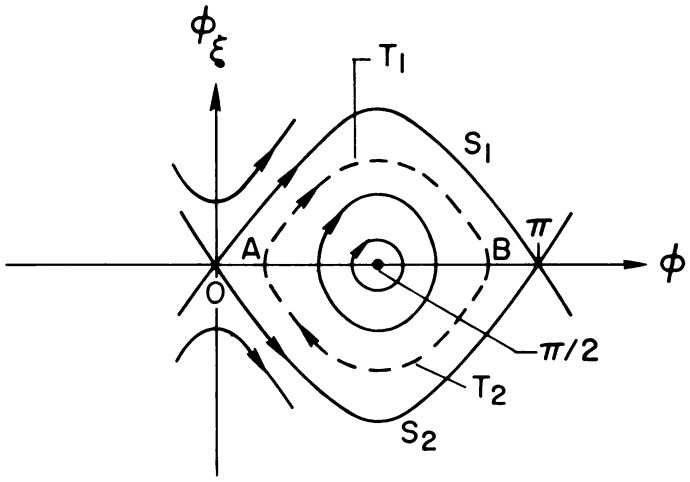


FIG. 4.1.

jectories correspond approaches

$$L_{\min} = \pi/(2b)^{1/2} \tag{4.15}$$

from above as the trajectories, as point sets, approach the point $\phi = \pi/2$, $\phi_\xi = 0$. This may be deduced from (4.14) or by linearizing the problem (4.12). Thus we have produced a family of solutions corresponding to all values of $L_b \geq L_{\min}$.

Of course there is an exactly corresponding family below the *$\phi$-axis*, between it and the separatrix $S_2$. More importantly however, we may observe that these two families of trajectories may be combined to produce still more physically different solutions. Such a solution consists of a finite concatenation of the form

$$\cdots T_1 T_2 T_1 T_2 \cdots . \tag{4.16}$$

Let $N_i$ denote the number of $T_i$, $i = 1, 2$ in this concatenation. Then the concatenation is a solution of the boundary value problem (4.12) provided

$$L_b = N_1 \oint_{T_1} d\xi + N_2 \oint_{T_2} d\xi \tag{4.17}$$

The constant solutions $\phi = 0$, $\pi/2$ and $\pi$ correspond to the rest points in the phase plane. These solutions are valid for all values of $L_b$. In particular, for

$$L_b \leq \pi/(2b)^{1/2}, \tag{4.18}$$

these are the only solutions which exist.

We assert that this constitutes all the solutions of the boundary value problem (4.12). Note that since (4.12) is invariant with respect to a change in the sign of $\xi$, we may identify certain pairs of these solutions as indistinguishable (viz. $T_1T_2$ and $T_2T_1$).

In Fig. 4.2, we schematize ($\phi$ versus $\xi$) the first family of solutions which we described, namely those of the form $T_1$. In this figure curves $\phi = \phi(\xi)$ corresponding to $T_1$ and $S_1$ in the phase plane are also labeled $T_1$ and $S_1$ respectively. The curve $E$ is the locus of endpoints of the family of curves corresponding to all $\{T_1\}$. The interval $[-L_{\min}, L_{\min}]$ on the $\xi$-axis corresponds to the constant solutions $\phi = \pi/2$.

In Fig. 4.3 we schematize the curve $\phi = \phi(\xi)$ corresponding to the concatenation

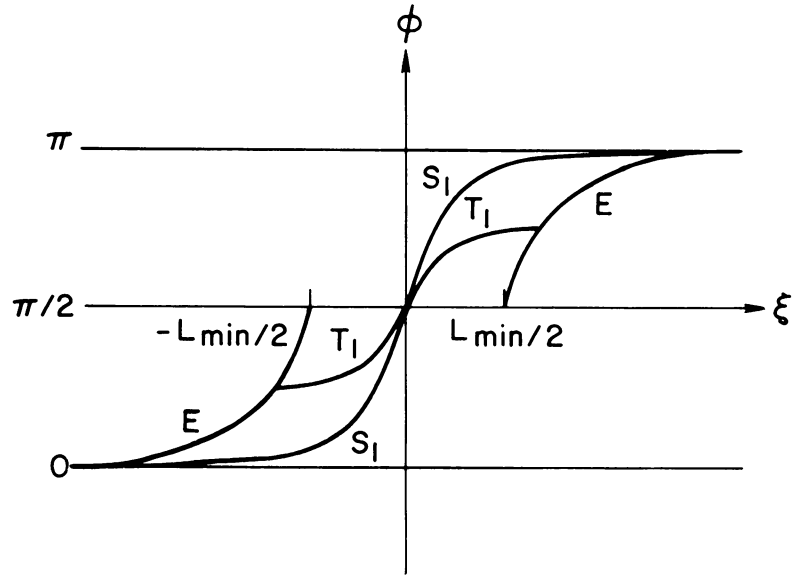


FIG. 4.2.

$T_1T_2T_1T_2T_1$ in order to suggest the physical form of the solutions represented by the class of concatenations which we have introduced. We observe a process of bifurcation. At integer multiples $n$ of $L_{\min}$ a nonconstant solution bifurcates from the $\phi = \pi/2$ constant solution. This bifurcating solution is a concatenation $\cdots T_1T_2 \cdots$, where

$$n = N_1 + N_2 \tag{4.19}$$

(Recall the identification of certain pairs of solutions previously made.) The corresponding bifurcation diagram is schematized in Fig. 4.4, where the ordinate may be viewed as the $L_2$ norm of $\phi(\xi, b) - \pi/2$.

*Domains and walls.* We now give a physical interpretation of the bifurcation diagram. For specimens where $L_b < L_{\min}$, only the constant solutions corresponding to the rest points $\phi = 0, \pi/2, \pi$, exist. The corresponding magnetization vector is uniform in the

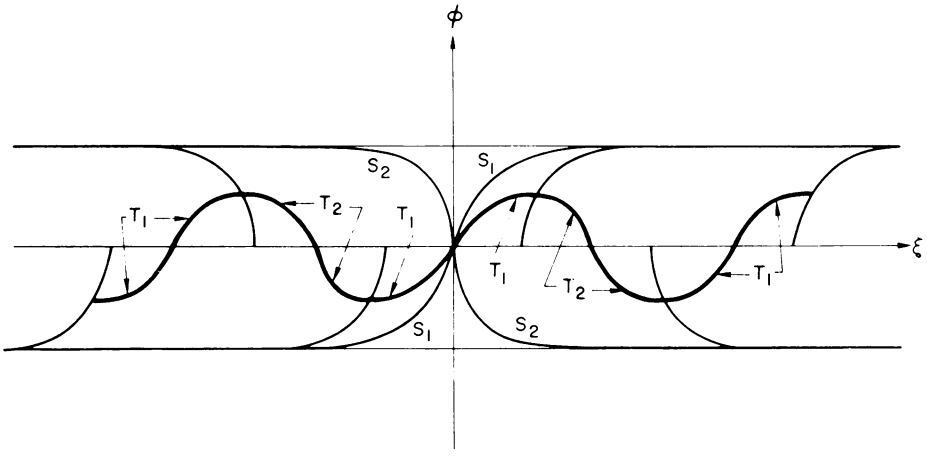


FIG. 4.3.

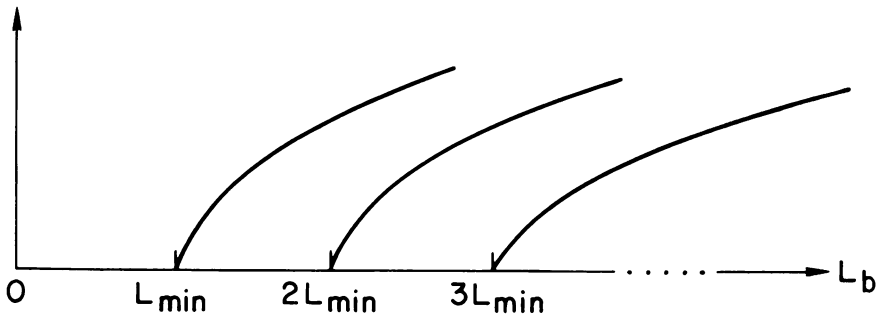


FIG. 4.4.

specimen. That is, the specimen consists of a single magnetic domain. According to the bifurcation diagram the possibility of a one-domain solution persists for all $L_b > 0$.

At $L_b = L_{\min}$ a solution of type $T_1$ bifurcates. As $\xi$ varies from $-b^{1/2}$ to $b^{1/2}$, $\phi$ passes from a region where it is approximately uniform, through $\pi/2$, to a region where it is once again approximately uniform. We interpret the regions of approximate uniformity of $\phi$ as magnetic domains. The intervening transition region we interpret as a domain wall. If $b^{1/2}$ is large so that $T_1$ approaches $S_1$, $\phi$ passes from a very large region where it is nearly zero to another very large region, where it is nearly $\pi$. Thus a solution of type $T_1$ corresponds to a specimen consisting of two domains separated by a domain wall.

Similarly at $L_b = nL_{\min}$ the solution of type $\cdots T_1T_2 \cdots$ which bifurcates corresponds to a specimen consisting of $n + 1$ domains separated correspondingly by $n$ walls.

Thus for $L \in (nL_{\min}, (n + 1)L_{\min})$ there are solutions corresponding to specimens exhibiting between one and $n + 1$ domains.

*Wall description.* To view the transition of the magnetization $\nu$ through a domain wall, it suffices to consider the variation of $\nu$ along $T_1$.

The three cases (1) $b > 0$, $\theta = 0$, (2) $b < 0$, $\theta = \pi$, (3) $b > 0$, $\theta = \pi/2$ give rise to a different wall geometries. The other possible cases are variants of these three.

1) $b > 0$, $\theta = 0$. Here (cf. (2.2))

$$\nu = \begin{bmatrix} \sin \phi(\xi) \\ 0 \\ \cos \phi(\xi) \end{bmatrix}, \tag{4.20}$$

where $\phi$ varies from $\pi/2$ − constant to $\pi/2$ + constant along $T_1$. Thus the wall behavior may be schematized as in Fig. 4.5.

2) $b < 0$, $\theta = \pi$,

$$\nu = \begin{bmatrix} -\cos \phi(\xi) \\ 0 \\ -\sin \phi(\xi) \end{bmatrix}. \tag{4.21}$$

Thus the wall behavior may be schenatized as in Fig. 4.6.

3) $b > 0$, $\theta = \pi/2$. Here

$$\nu = \begin{bmatrix} 0 \\ \sin \phi(\xi) \\ \cos \phi(\xi) \end{bmatrix}. \tag{4.22}$$

The wall behavior may be schematized as in Fig. 4.7.

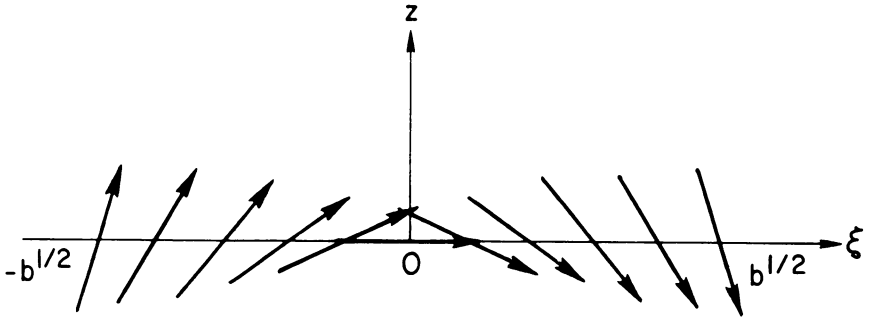


FIG. 4.5.

Example 2. In this example we take

$$f(\theta, \phi) = \begin{cases} k_{11} \sin^2\phi + k_{12} \cos^2\phi, & x \in (-1,0), \\ k_{21} \sin^2\phi + k_{22} \cos^2\phi, & x \in (0,1). \end{cases} \tag{4.23}$$

Using (4.1)–(4.3), the boundary value problem (3.7)–(3.9) becomes

$$\frac{d^2\phi}{dx^2} - \sin 2\phi \left(\frac{d\theta}{dx}\right)^2 - \mu\pi \sin 2\phi \cos^2\theta + \sin 2\phi \begin{cases} \lambda(k_{12} - k_{11}) \\ \lambda(k_{22} - k_{21}) \end{cases} = 0, \qquad x \in \begin{cases} (-1,0) \\ (0,1) \end{cases}, \tag{4.24}$$

$$\sin^2\phi \frac{d^2\theta}{dx^2} + \sin^2\phi \frac{d\theta}{dx} \frac{d\phi}{dx} + \mu\pi \sin^2\phi \sin^2\theta = 0, \qquad x \in (-1,1), \tag{4.25}$$

and

$$d\phi/dx = 0, \qquad \sin^2\phi(d\theta/dx) = 0, \qquad x = \pm 1. \tag{4.26}$$

Let

$$\xi = \lambda^{1/2} x \tag{4.27}$$

and set

$$a = k_{11} - k_{12}, \qquad b = k_{21} - k_{22}. \tag{4.28}$$

This boundary value problem has solutions $\theta = 0, \pi/2, \pi$ and $3\pi/2$ where $\phi = \phi(x)$. Let

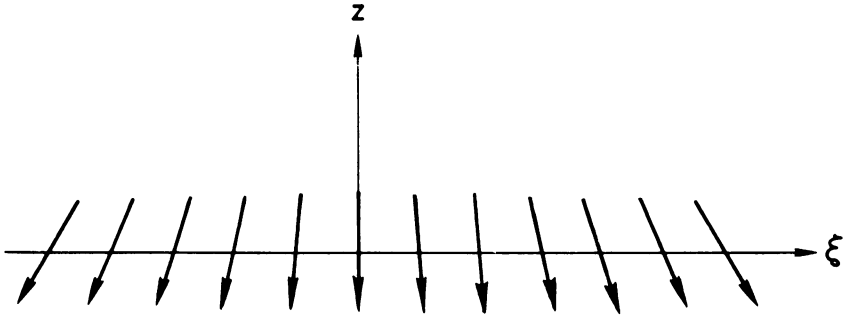


FIG. 4.6.

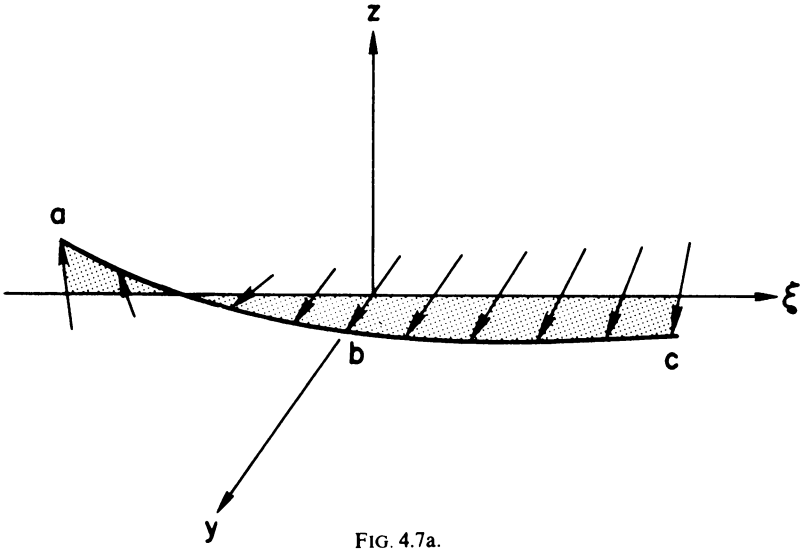


FIG. 4.7a.

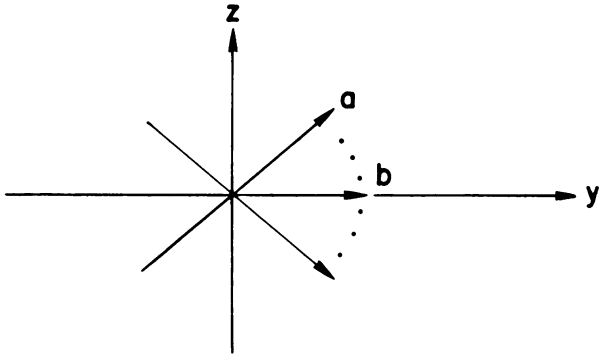


FIG. 4.7b. The wall of Fig. 4.7a projected onto the $yz$-plane.

us restrict our attention to the case $\theta = \pi/2$. In this case $\phi(x)$ is a solution of this following boundary value problem:

$$\frac{d^2\phi}{d\xi^2} = \left.\begin{matrix} a \\ b \end{matrix}\right\} \sin 2\phi, \ \xi \lesseqgtr 0, \tag{4.29}$$

$$d\phi/d\xi = 0, \qquad \xi = \pm\lambda^{1/2}. \tag{4.30}$$

Let us suppose for convenience that $a > 0$ and $b < 0$. The differential equation (4.29) written with $a$ or with $b$ alone has a $(\phi, \phi_\xi)$-phase plane which we call the $a$-plane or the $b$-plane respectively. The $a$-plane is qualitatively the same as the one in Fig. 4.1. The same is true for the $b$-plane except that it is shifted $\pi/2$ to the left. Of course the two planes are distorted vertically with respect to each other.

A solution of the boundary value problem starts on the interval $\phi \in [0, \pi]$ in the $a$-plane and moves until

$$\oint d\xi = \lambda^{1/2}. \tag{4.31}$$

Then the solution transfers to a trajectory in the $b$-plane returning to the $\phi$-axis therein. The transit in the $b$-plane also obeys (4.31).

We can supplement this qualitative description of the solutions of the boundary value problem by a more detailed and quantitative one. To do this we proceed with the following phase plane analysis.

The orbits in the $a$- and $b$-planes which enclose the points $(\pi/2, 0)$ and $(0,0)$ respectively, have values of $\oint d\xi$ which are bounded below respectively by

$$L_{\min a} = \pi \left(\frac{2}{|a|}\right)^{1/2}, \qquad L_{\min b} = \pi \left(\frac{2}{|b|}\right)^{1/2}. \tag{4.32}$$

The boundary value problem (4.29) and (4.30) is defined on an interval of length $2\lambda^{1/2}$ with a length of $\lambda^{1/2}$ for each of its portions ($\xi \lesseqgtr 0$). For convenience we suppose that

$$\lambda^{1/2} > \frac{1}{2} \min (L_{\min a}, L_{\min b}) = \frac{\pi}{\sqrt{2}} \min (a^{-1/2}, |b|^{-1/2}). \tag{4.33}$$

In Figs. 4.8(i) and (ii) respectively, we schematize two families of the parts of the trajectories in the $a$-plane which correspond to the solution of the boundary value problem (4.29) and (4.30) for $\xi < 0$.

In Figs. 4.9(i) and 4.9(ii), we indicate the locus of the endpoints of the families of curves in Figs. (4.8). These loci are spirals, called $S_a^1$ and $S_a^2$ respectively. $S_a^1$ and $S_a^2$ respectively emanate from the saddle points (0, 0), $(\pi, 0)$ respectively and terminate with a finite number of windings at the rest point $(\pi/2, 0)$. The points on the interval $[0, \pi/2]$ of the $\phi$-axis where $S_a^1$ crosses are numbered consecutively beginning with zero at the saddle point. Correspondingly, we number the points in $[\pi/2, \pi]$ relative to $S_a^2$ (see Figs. 4.9 (i) and 4.9 (ii)). We call these numbers $C_0^a$, $C_1^a$, $\cdots$, suppressing their dependence on the particular spiral $S_a^1$ or $S_a^2$ since no confusion should occur. The portion of the spiral $S_a^1$ which goes from $C_i^a$ to $C_j^a$ is called $S_a^1(C_i^a C_j^a)$; similarly for $S_a^2(C_i^a C_j^a)$. Actually we will only make use of the case $C_j^a = C_{i+1}^a$. For such portions of the spiral we simply write $S_a^{1,2}(C_i^a, C_{i+1}^a)$ as $S_a^{1,2}(C_i^a)$, respectively.

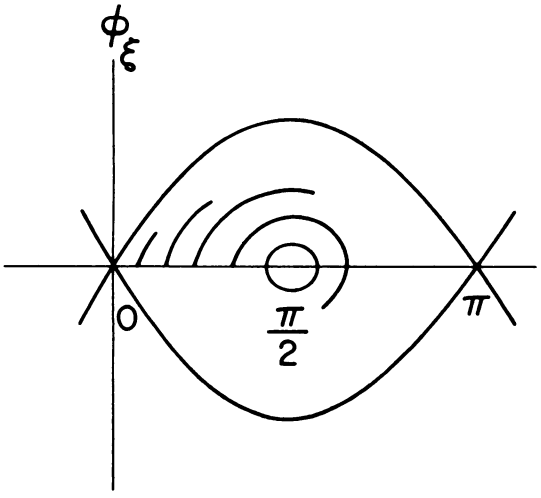


FIG. 4.8(i).

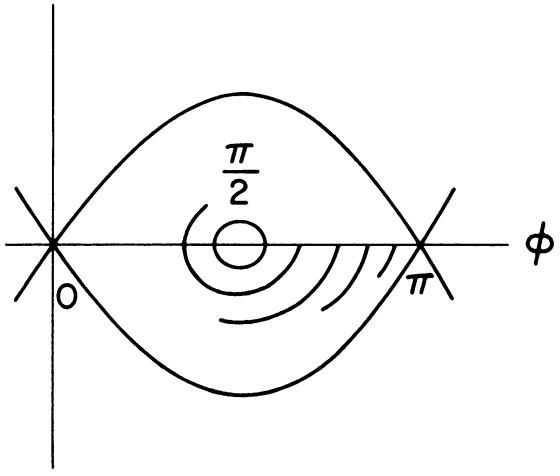


FIG. 4.8(ii).

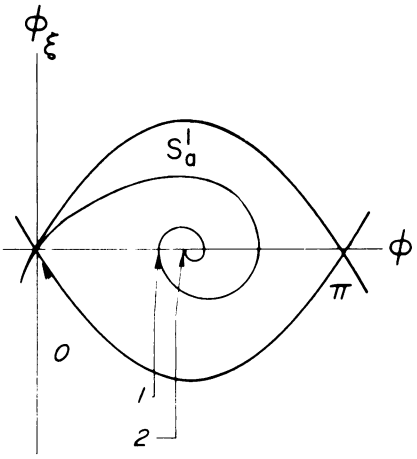


FIG. 4.9(i).

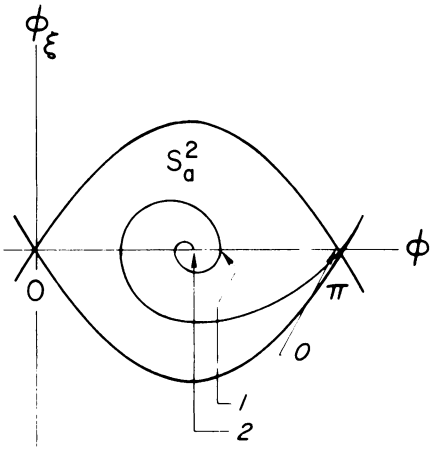


FIG. 4.9(ii).

The portions $S_a{}^1(C_i^a)$ have the following geometrical significance. They are the loci of the ends of trajectories (as described and indicated in Fig. 4.8) which in particular wind around the rest point $C_i^a$ times (but less than $(C_i^a + 1)$-times); similarly for the portions of $S_a{}^2(C_i^a)$.

Now we pass to the $b$-plane and we consider the sets of trajectories analogous to the ones described in the $a$-plane. Here, however, we imagine $\xi$ to run backwards. That is, we are interested in trajectory portions which terminate on the $\phi$-axis, and which are run backwards (with respect to $\xi$) until they satisfy the condition $\oint d\xi = \lambda^{1/2}$. Here however, we must consider four families and four spirals, all of which are qualitatively analogous to the ones already described in the $a$-plane. In Figs. 4.10(i) and 4.10(ii) we indicate the appropriate spirals $S_b^i$, $i = 1, 2, 3, 4$. The appropriate crossings of these new spirals with the $\phi$-axis are labeled as before and they define correspondingly portions $S_b{}^i(C_l^b, C_m{}^b)$, $i = 1, 2, 3, 4$; $C_l^b$, $C_m{}^b = 0, 1, \cdots$ . Similarly, we introduce the shorter notation for the segments $S_b{}^i(C_j^b)$, $i = 1, 2, 3, 4$ which have the corresponding meaning as above for the windings of trajectories. These spirals, etc. are illustrated in Figs. 4.10(i) and 4.10(ii).

We note that as $\lambda^{1/2}$ increases all the spirals grow in the sense of acquiring more windings themselves. As $\lambda^{1/2}$ decreases the spirals unwind until they are completely unwound; each coinciding with a portion of the $\phi$-axis between the two rest points which are a spiral's termini.

Now we may describe in a more detailed manner the collection of solutions of the boundary value problem (4.29) and (4.30) which were described qualitatively above.

For given values of $a$, $b$ and $\lambda^{1/2}$ we superpose the $a$- and $b$-phase planes. (Imagine Figs. 4.9(i), 4.9(ii), 4.10(i) and 4.10(ii) to be superposed.) Every intersection point of a spiral $S_a^i$, $i = 1, 2$ with a spiral $S_b^j$, $j = 1, 2, 3, 4$ defines a solution of the boundary value problem. Suppose for example that one of these intersections, $P$, occurs along $S_a{}^1(0)$ and $S_b{}^3(1)$. Then the solution in question corresponds to the trajectory in the $a$-plane which emanates from the interval $[0, \pi/2]$ on the $\phi$-axis (ascending above it) and reaches $P$ on $S_a{}^1$ (without winding around the rest point $(\pi/2, 0)$). Then the solution follows the trajectory in the $b$-plane starting at $P$, winding around the rest point $(0, 0)$ once and then terminating at a point in the interval $[0, \pi/2]$ on the $\phi$-axis.

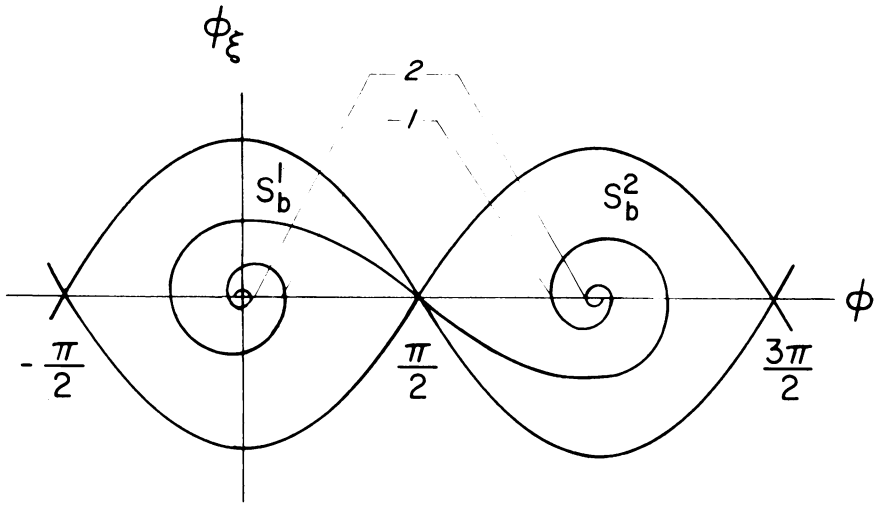


FIG. 4.10(i).

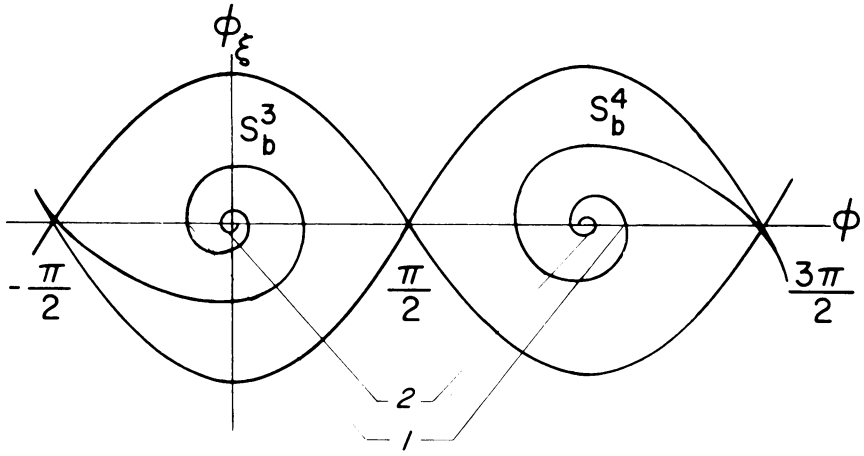


FIG. 4.10(ii).

We plot this solution description in Fig. 4.11(i) for the phase plane and in Fig. 4.11(ii) in the $(\xi, \phi)$ plane. The segment $S_b^3$ (1) is in a heavy line. The portion of the solution in the $a$-plane is the dotted curve starting at $s$ and terminating at $P$. The portion of the solution in the $b$-plane is the dotted curve starting a $P$ and proceeding to $t$, $a$, $b$, $c$ and back to $P$ and then to $t$ where it terminates. The points $s$, $P$, $a$, $b$, $c$ and $t$ in the $\phi = \phi(\xi)$ plot correspond to the points in the phase planes labeled correspondingly.

Using the terminology of the section of walls and domains in the previous example, we see that the special solution illustrated in Fig. 4.11(ii) corresponds to a magnetic state consisting of three domains separated by two walls.

The rest points $(0, 0)$, $(\pi/2, 0)$, $(\pi, 0)$ lie on a spiral in both the $a$- and $b$-planes and so these rest points are solutions for all values of $\lambda^{1/2}$. They represent the constant solutions $\phi = 0, \pi/2, \pi$.

Since every intersection $P$ of spirals in $a$- and in $b$-planes corresponds to a solution of the boundary value problem, we see that the larger $\lambda^{1/2}$ is (and with it the more winds

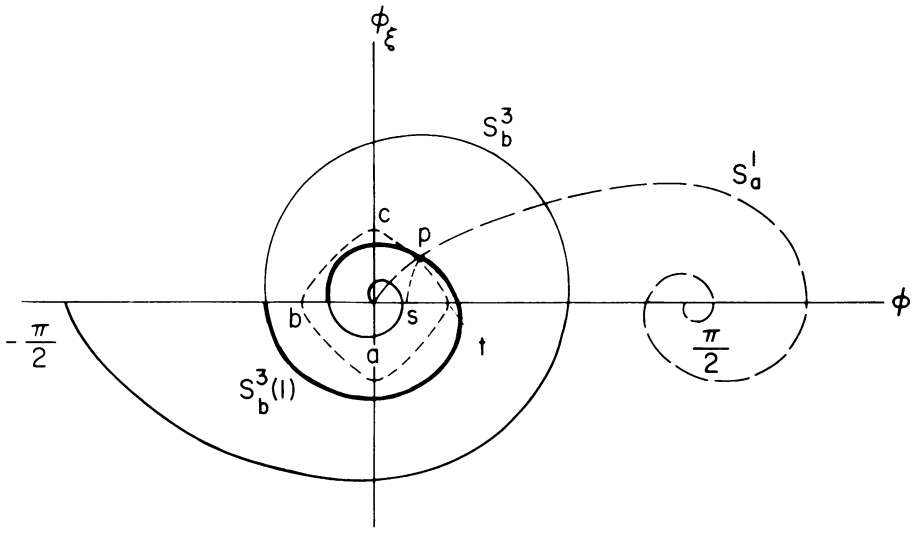


FIG. 4.11(i).

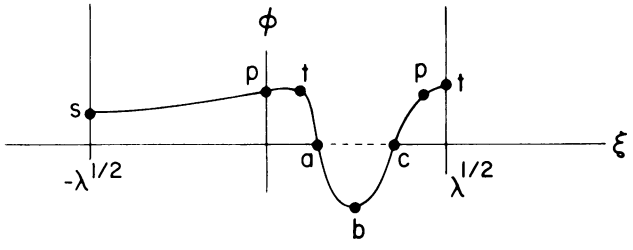


FIG. 4.11(ii).

there are of the spirals) the greater is the number of solutions. When $\lambda^{1/2}$ decreases we have observed that the spirals unwind. As $\lambda^{1/2}$ approaches zero the spirals are completely unwound and they collapse into segments of the $\phi$-axis.

We have not analyzed the collection of solutions of Example 2 sufficiently to indicate the bifurcation process in the form of a diagram of the nature of Fig. 4.4. We forego as well an enumeration of solution types giving rise to the different wall types as in Figs. 4.5, 4.6 and 4.7.

*Stability considerations.* Of the many solutions presented in Examples 1 and 2, the ones which correspond to minima of $\bar{E}_{Tot}$ represent domain configurations which may arise physically.

Since in the examples $\theta$ = const and $\phi = \phi(x)$, the expression for $\delta^2\bar{E}_{Tot}$ becomes (cf. (3.14))

$$\delta^2\bar{E}_{Tot} = \int_{-1}^{1} \left\{\lambda\left[\frac{1}{2} f_{\theta\theta}(\delta\theta)^2 + f_{\theta\phi}\delta\theta\delta\phi + \frac{1}{2} f_{\phi\phi}(\delta\phi)^2\right]\right.$$

$$-\pi\mu[\sin^2\phi \cos 2\theta(\delta\theta)^2 - \cos^2\theta \cos 2\phi(\delta\phi)^2 + \sin 2\theta \sin 2\phi\delta\theta\delta\phi]$$

$$\left. + \frac{1}{2}[(\nabla\delta\phi)^2 + \sin^2\phi(\nabla\delta\theta)^2]\right\} dx \qquad (4.34)$$

where we have specialized the variations to be functions only of $x$.

Example 1. In the case of Example 1, the expression (4.34) for $\delta^2\bar{E}_{Tot}$ becomes

$$\delta^2\bar{E}_{Tot} = \int_{-1}^{1} \Big\{(\delta\theta)^2[(\lambda\gamma - \pi\mu)\sin^2\phi\cos 2\theta] + \delta\theta\delta\phi[(\lambda\gamma - \pi\mu)\sin 2\theta \sin 2\phi] + (\delta\phi)^2[\cos 2\phi(-\lambda + \pi\mu\cos^2\theta + \lambda\gamma\sin^2\theta)] + \frac{1}{2}[(\nabla\delta\phi)^2 + \sin^2\phi(\nabla\delta\theta)^2]\Big\}\, dx. \quad (4.35)$$

Conditions on the parameters $\gamma$, $\lambda$ and $\mu$ for which the constant solutions to the boundary value problem (4.5)–(4.7) are stable (i.e. when $\delta^2\bar{E}_{Tot} > 0$) are given in Table 1. (Note that the closure of the union of the domains in $(\gamma, \lambda, \mu)$-space defined by the conditions in this table is indeed all of $(\gamma, \lambda, \mu)$ space.)

A study of these conditions shows that the constant solutions which correspond to rest points which are centers in the plane are always unstable. This implies that the bifurcated solutions close to the centers in the phase plane are always unstable. In terms of the bifurcation diagram of Fig. 4.4, this means that the entire branch corresponding to the $L_b$-axis as well as a beginning portion of each ascending branch correspond to unstable solutions. The state of stability of the upper portions of the ascending branches is yet to be determined.

Example 2. In the case of Example 2, the expression (4.34) for $\delta^2\bar{E}_{Tot}$ becomes (recall we are studying the particular case when $\theta = \pi/2$ in this example (cf. Eq. (4.28) ff.)),

$$\delta^2\bar{E}_{Tot} = \int_{-1}^{0} \lambda a\cos^2\phi(\delta\phi)^2 dx + \int_{0}^{1} \lambda b\cos^2\phi(\delta\phi)^2 dx + \int_{-1}^{1} \pi\mu\sin^2\phi(\delta\theta)^2 dx + \frac{1}{2}\int_{-1}^{1}((\nabla\delta\phi)^2 + \sin^2\phi(\nabla\delta\theta)^2) dx. \quad (4.36)$$

Consider the constant solutions $\phi = 0, \pi/2$ and $\pi$. If $ab < 0$ there exist variations $(\delta\theta, \delta\phi)$ such that $\delta^2\bar{E}_{Tot} < 0$ for $\lambda$ sufficiently large. Thus the constant (one-domain) solutions are unstable. Then there must exist non-constant stable solutions of the magnetic domain problem. If indeed these stable solutions lie among those of the form $(\theta, \phi) = (\pi/2, \phi(x))$ which we produced, we have the existence of stable multidomian solutions.

*Remark.* As we noted in the introduction, we see that while many of the non-constant (i.e. multidomain) solutions which we have produced are not stable, they do exhibit the solution structures which are observed experimentally. We conjecture that some of our solutions are stable while others may be stabilized by simple means such as adding an appropriate applied magnetic field.

TABLE 1.

| $\phi$ | $\theta$ | Conditions |
|---|---|---|
| $0, \pi$ | $\forall\theta$ | $\pi\mu > \lambda, \gamma > 1$ |
| $\pi/2$ | $0, \pi$ | $\lambda\gamma > \pi\mu, \lambda > \pi\mu$ |
| $\pi/2$ | $\pi/2$ | $\pi\mu > \lambda\gamma, \gamma > 1$ |

However, the point to this work is to show that the manifold of different states of magnetism observed experimentally is connected by the standard mathematical process of bifurcation, thereby giving a global structure to this set of solutions.

## References

[1] W. F. Brown, Jr., *Micromagnetics,* Interscience, New York (1963)
[2] H. Chang, *Magnetic bubble technology,* IEEE Press, New York (1975)
[3] T. H. O'Dell, *Magnetic bubbles,* J. Wiley & Sons, New York (1974)
[4] J. D. Jackson, *Classical electrodynamics,* J. Wiley & Sons, New York (1975)
[5] G. A. Jones and B. K. Middleton, *A review of domain wall models in thin magnetic films,* Int. J. Magnetism **6**, 1–18 (1974)
[6] A. H. Bobeck and E. Della Torre, *Magnetic bubbles,* North-Holland Publishing Company, Amsterdam (1975)